

## Effect of Aluminum on Nitroform - A DFT Study

Lemi Türker

Department of Chemistry, Middle East Technical University, Üniversiteler, Eskişehir Yolu No: 1, 06800 Çankaya/Ankara, Turkey; e-mail: lturker@gmail.com; lturker@metu.edu.tr

### Abstract

Trinitromethane (nitroform, NF) is an interesting substance. It acts as an oxidizer and forms salts/salt-like materials. In the present study, nitroform and aluminum interaction has been investigated within the limitations of density functional theory at the level of unrestricted B3LYP/6-311++G(d,p). The composites having formula of NF+Al and NF+2Al are considered. Since aluminum has an unpaired electron in the ground state, various multiplicities arise for the composites of present interest. Some geometrical, physico chemical, quantum chemical and spectral data have been obtained and discussed. The results indicate that the interaction between aluminum and nitroform is moderate in the case of NF+Al(d) which (has doublet multiplicity) and only some bond angle and length distortions happen. In the case of NF+2Al(s) composite, drastic effect of aluminum atom results in C-NO<sub>2</sub> bond rupture of nitroform. On the other hand, the triplet state of NF+2Al, (NF+2Al(t)) perturbations caused by the aluminum is also moderate. In each case the aluminum atom acquires partial positive charge.

### 1. Introduction

Trinitromethane (nitroform) and its salts have been known for almost more than a century (The salt of nitroform and hydrazine, hydrazinium nitroformate (HNF), was reported to be discovered in 1951) [1]. In the literature, numerous publications exist on nitroform salts but relatively less number of articles piled on nitroform [2-9]. Soon after its discovery, it was recognized that HNF belongs to the most powerful solid oxidizers in existence and considerable attempts have been made to use HNF as a propellant ingredient in high energy solid propellants [2-9] and are the subject of several structure-related publications [10], including an *ab initio* study predicting a propeller-type structure

Received: May 22, 2022; Accepted: June 11, 2022

Keywords and phrases: nitroform; aluminum; explosive; oxidizers; DFT.

Copyright © 2022 Lemi Türker. This is an open access article distributed under the Creative Commons Attribution License (<http://creativecommons.org/licenses/by/4.0/>), which permits unrestricted use, distribution, and reproduction in any medium, provided the original work is properly cited.

for the anion (nitroformate) [11]. Xiao and coworkers investigated the intermolecular interaction of hydrazinium nitroformate ion pair by using density functional theory [12]. Hydrazinium nitroformate (HNF) is an energetic oxidizer [13-15]. It is used to produce propellants which burn very rapidly, exhibiting very high combustion efficiency. Its high energy leads to propellants having high specific impulse.

Substantial efforts were directed to HNF synthesis and stabilization, and to methods to control the HNF crystal particle size [3-6]. In the early seventies HNF research was suddenly stopped. One of the major reasons for this: the hazardous synthesis method of nitroform. Several fire and explosion accidents have been reported that forced to stop nitroform production, and subsequently HNF synthesis [2]. Another hindrance was the incompatibility between HNF and some important binders like hydroxy-terminated polybutadiene (HTPB). However, some safe synthesis method for HNF has been established, starting from nitroform and hydrazine. Nowadays, there are safe ways to manufacture nitroform [16-18] (e.g., the Rockwell method).

Many scientists and companies developed new energetic compounds and powerful oxidizers like hexanitroethane, nitronium perchlorate, hydrazinium mono- and diperchlorates, hydroxylamine perchlorate, hydrazinium nitroformate, dioramino compounds, fuels like boron, metal hydrides, and metals like beryllium and zirconium [19-21]. Aluminum has been used for several decades in certain TNT/NH<sub>4</sub>NO<sub>3</sub> commercial explosives (e.g., the Ammonals) as an additional fuel to increase the power and gas volume. Aluminized military explosives appeared as prominent charges in II World War [22].

Aluminum powder is one of the combustible high energy materials. Hence, it influences the explosive performance by increasing the heat of explosion and acts as intermediate sensitive agent [23]. As an overall effect it enhances reaction temperature and air blast, increases bubble energies in underwater weapons etc. It is known that pressed samples of 80% HNF and 20% aluminum have an increased burning rate as compared to neat HNF whereas the burning rate exponent remains similar to the HNF pellets. The high HNF flame temperature close to the surface (0.5 mm above the surface) together with the high OH concentration leads to a very effective aluminum combustion. Ultra fine aluminum powder (Alex) (20%) yields further enhanced burn rates with HNF (80%) and a reduced burning rate exponent (approximately 0.7). HNF together with energetic binders and aluminum, yields propellants with very high specific impulses (> 3100 m/s) [6].

Although, some work exist in the literature involving HNF and aluminum compositions in certain ammunitions, the effect of aluminum on nitroform, basic constituents of HNF, has not been published so far up to the best knowledge of the author. In the present study, interaction of nitroform with aluminum has been investigated at the molecular level within the limitations of density functional theory (DFT).

## 2. Method of Calculation

In the present study, the initial geometry optimizations of all the structures leading to energy minima were achieved by using MM2 method then followed by semi-empirical PM3 self-consistent fields molecular orbital (SCF MO) method [24,25] at the restricted level [26]. Afterwards, the structure optimizations have been managed within the framework of Hartree-Fock (HF) and finally by using density functional theory (DFT) at the unrestricted level of B3LYP/6-311++G(d,p) [27,28]. Note that the exchange term of B3LYP consists of hybrid Hartree-Fock and local spin density (LSD) exchange functions with Becke's gradient correlation to LSD exchange [29]. Also note that the correlation term of B3LYP consists of the Vosko, Wilk, Nusair (VWN3) local correlation functional [30] and Lee, Yang, Parr (LYP) correlation correction functional [31]. Presently, to minimize the basis set superposition error (BSSE) rather high level of basis set has been employed [26,32]. In the present study, the normal mode analysis for each structure yielded no imaginary frequencies for the  $3N-6$  vibrational degrees of freedom, where  $N$  is the number of atoms in the system. This indicates that the structure of each molecule corresponds to at least a local minimum on the potential energy surface. Furthermore, all the bond lengths were thoroughly searched in order to find out whether any bond cleavage occurred or not during the geometry optimization process. All these computations were performed by using SPARTAN 06 [33].

## 2. Results and Discussion

Nitroform (NF, trinitromethane) is the basic constituent of HNF and some other nitroform salts [6,9,10,34]. It can exist in two tautomeric forms; a nitroform and an *aci*-form. The colorless nitroform exists in solution acidified with HCl or H<sub>2</sub>SO<sub>4</sub> and also in anhydrous benzene, CS<sub>2</sub> and ether [1]. Whereas, in aqueous and basic solutions, which are intensely yellow colored, nitroform partly turns into the *aci* tautomeric form.

On the other hand, aluminum which takes part as an important ingredient of many explosive compositions [35] has the ground state electronic configuration of  $1s^2 2s^2 2p^6 3s^2 3p^1$  [36]. Thus, it is capable of donating electrons and/or accepting lone

pair(s) to form complexes. In the present study composites having formulas of NF+Al and NF+2Al are considered which possess 15.15 and 26.32 % Al by weight, respectively. Note that those composites possess doublet state in NF+Al and singlet or triplet in NF+2Al case.

Figure 1 shows the optimized structures as well as the directions of the dipole moment vectors of nitroform (NF) and its aluminized forms. As seen in the figure, nitroform has a propeller type arrangement of the nitro groups with C<sub>1</sub> symmetry. The direction of dipole moment vector is from the hydrogen atom through the carbon atom. Presence of the aluminum atom perturbs nitroform structure at different extents depending on the number of the aluminum atom(s) and the multiplicity of the systems considered. Note that aluminum atom has an unpaired electron thus at the unrestricted level of calculations various multiplicities arise as the number of Al atoms varies.

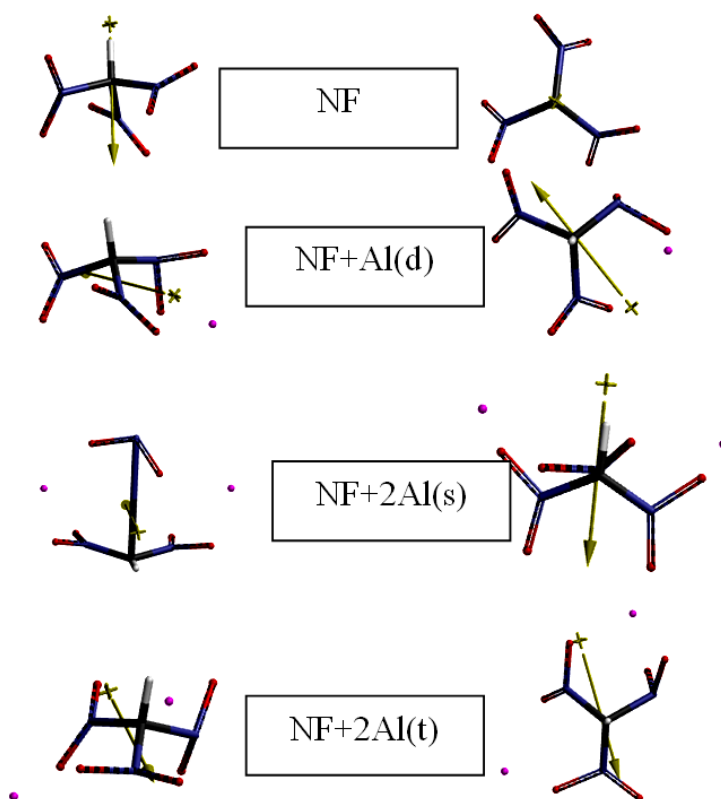


**Figure 1.** Optimized structures of nitroform and its aluminized forms (From different angles of views).

In the case of NF+2Al(s) composite, drastic effect of aluminum atom results in C-NO<sub>2</sub> bond rupture of nitroform. In the other cases the perturbations are in the form of some bond angle and length distortions but no bond cleavages.

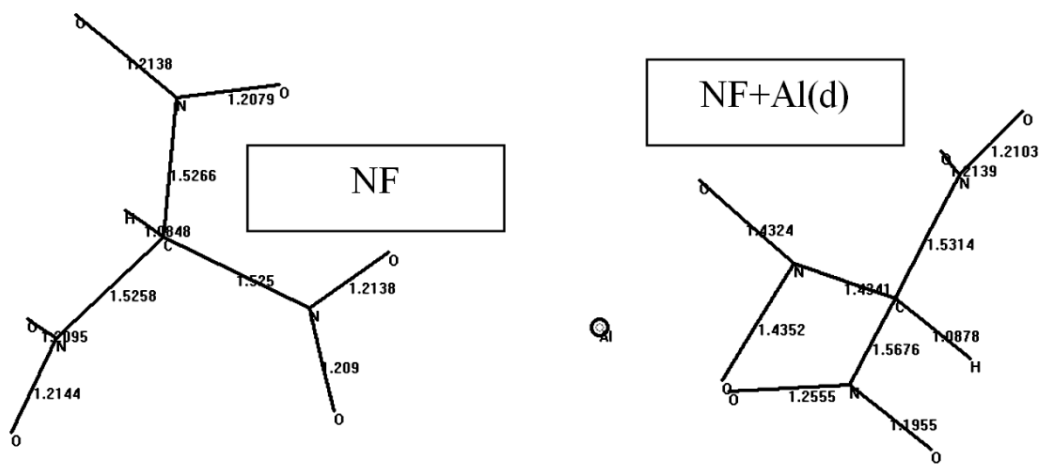
Table 1 shows the dipole moment components and the total dipole moments of the composites. As seen in Table 1 the order of dipole moments is NF+2Al(s) < NF+Al(d) < NF+2Al(t). Apparently the open shell structures have greater total dipole moments than the closed-shell structure, NF+2Al(s). Obviously the magnitude of dipole moments have been dictated by the geometric factors as well as the charges of the atomic centers of the systems considered (see Figures 2 and 3).

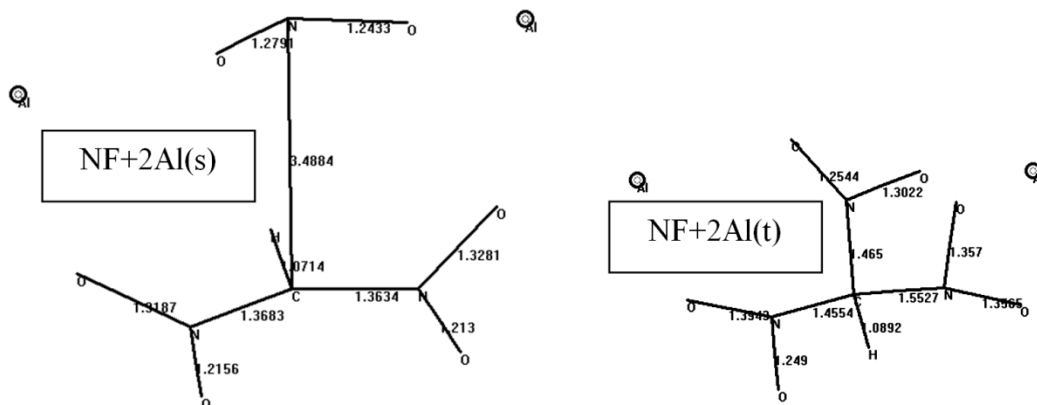
**Table 1.** Dipole moment components and the total dipole moments of the composites.

Composite	X	Y	Z	Total
NF+Al(d)	-1.556620	-2.714519	0.222418	3.137061
NF+2Al(s)	1.654220	1.978691	1.477984	2.972557
NF+2Al(t)	-4.273328	1.156174	-0.855965	4.508963

In debye units.

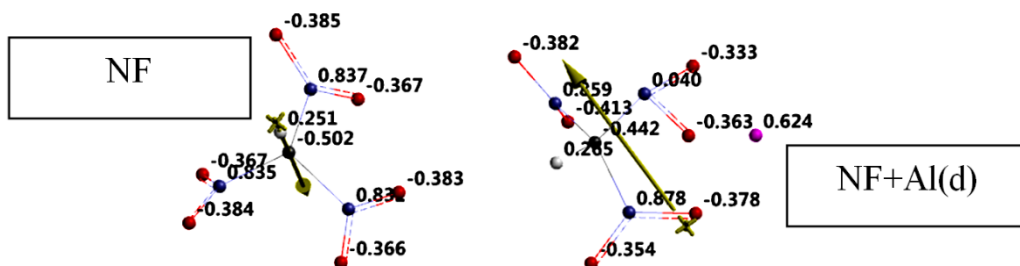
Figure 2 shows the calculated bond lengths in the systems considered. As seen in the figure, drastic effect of aluminum atom occurs in the case of NF+2Al(s) composite which results in C-NO<sub>2</sub> bond rupture of nitroform. As mentioned above, in the other cases the perturbations are relatively much less and only some bond angle and length distortions happen.

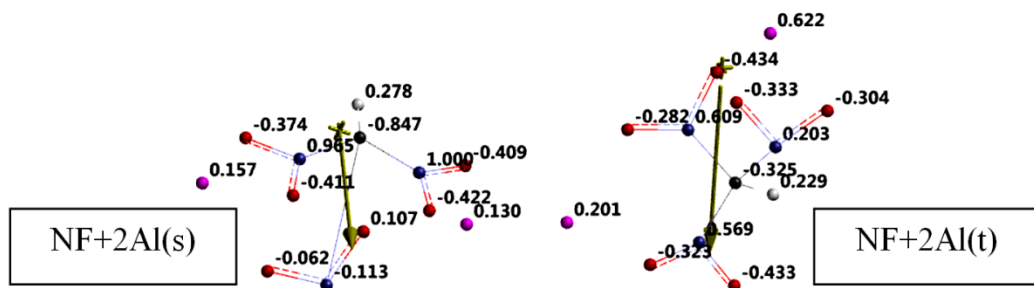




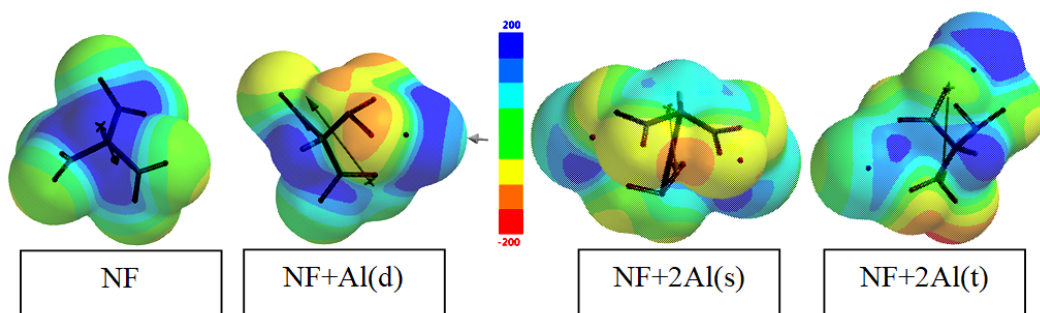
**Figure 2.** Calculated bond lengths in the systems considered.

Figure 3 displays the calculated electrostatic potential (ESP) charges on atoms of the systems considered. Note that the ESP charges are obtained by the program based on a numerical method that generates charges that reproduce the electrostatic potential field from the entire wavefunction [33]. As seen in Figure 3, the aluminum atoms are all partially positively charged in the composites. The greatest charge on the aluminum occurs in NF+Al(d) composite but if sum of the charges on Al atoms in each composite are considered the order is NF+2Al(t) > NF+Al(d) > NF+2Al(s). In the composites, the electron population transferred to nitroform is spread over the whole nitroform molecule, thus the electrostatic potential maps of the composite systems considered are highly different from the respective map of nitroform (Figure 4). Note that the overall negative charge of the NO<sub>2</sub> moiety removed from NF+2Al(s) composite is very small. In the composites, the carbon atom has some negative partial charge and the negative charge accumulated on the carbon atom in NF+2Al(s) case (from which the NO<sub>2</sub> group is removed) is the most negative of all, including the nitroform molecule itself.





**Figure 3.** The calculated ESP charges on atoms of the systems considered.



**Figure 4.** The electrostatic potential maps of the systems considered.

Figure 5 displays the calculated IR spectra of the systems considered. Nitroform spectrum is characterized with two adjacent peaks at  $1674\text{ cm}^{-1}$  and  $1673\text{ cm}^{-1}$  which are asymmetric N-O stretchings overlapped with C-NO<sub>2</sub> bendings. The peak at  $1348\text{ cm}^{-1}$  stands for symmetric N-O stretching. The C-H stretching of nitroform occurs at  $3194\text{ cm}^{-1}$ . The presence of Al in NF+Al(d) composite slightly shifts asymmetric N-O stretchings to  $1664\text{ cm}^{-1}$  and  $1640\text{ cm}^{-1}$  again overlapped with C-H vibrations. The C-H stretching and bending occurs at  $3166\text{ cm}^{-1}$  and  $1333\text{ cm}^{-1}$ ,  $1271\text{ cm}^{-1}$ , respectively. In the case of NF+2Al(s), the C-H stretching happens at  $3328\text{ cm}^{-1}$ . At  $1598\text{ cm}^{-1}$  asymmetric N-O stretchings overlapped with C-NO<sub>2</sub> bendings occur. The intense sharp peaks at  $1409\text{ cm}^{-1}$  and  $1210\text{ cm}^{-1}$  belong to the C-H bending coupled with asymmetric N-O stretchings of the eliminated NO<sub>2</sub> moiety. As for the NF+2Al(t) composite C-H stretching occurs at  $3137\text{ cm}^{-1}$ . The peaks at  $1413\text{ cm}^{-1}$  and  $1394\text{ cm}^{-1}$  are asymmetric N-O stretchings coupled with C-N bendings. The intense peak at  $964\text{ cm}^{-1}$  arises from the asymmetric stretchings of N-O bonds of some other NO<sub>2</sub> groups.

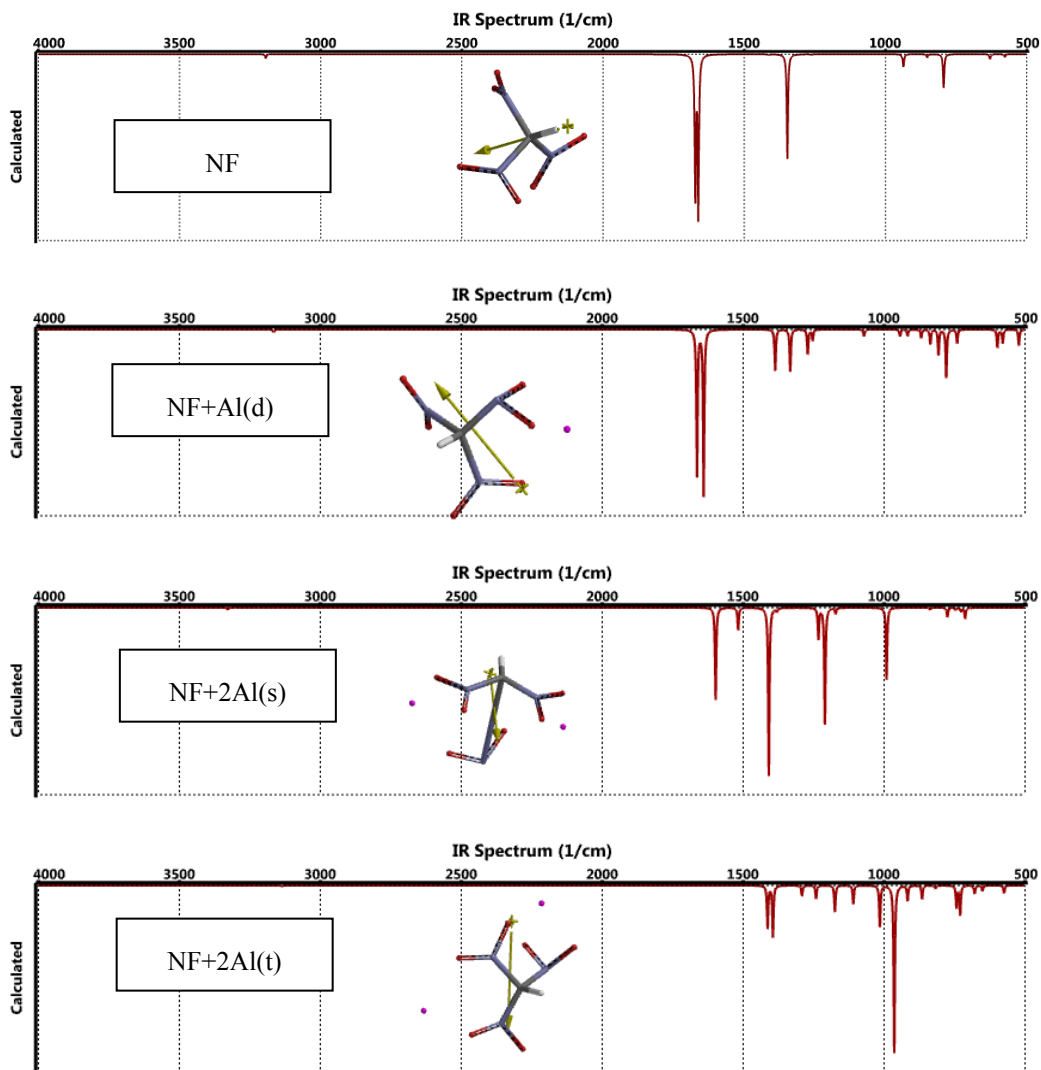


**Figure 5.** Calculated IR spectra of the systems considered.

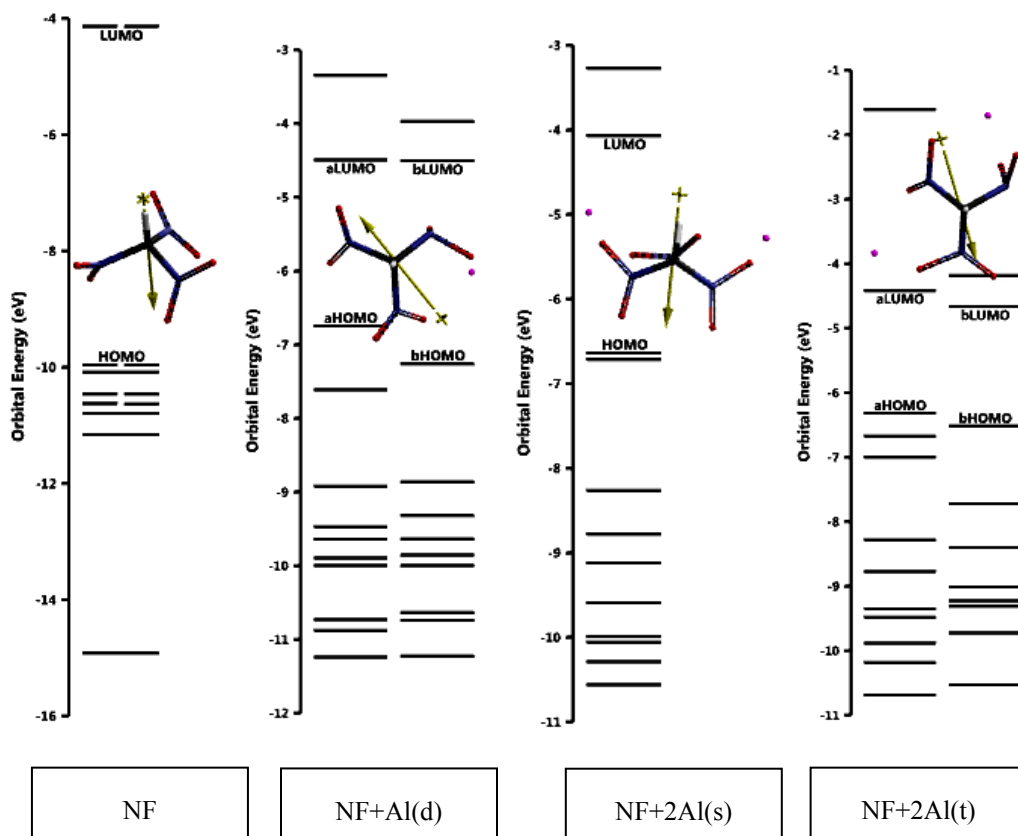
Table 2 shows some energies of the composites considered where  $E$ , ZPE and  $E_C$  stand for the total electronic energy, zero point vibrational energy and the corrected total electronic energy, respectively. The data indicate that of the two NF+2Al composites, the singlet is more stable than the triplet. However, note that the singlet has a decomposed nitroform structure.

**Table 2.** Some energies of the composites considered.

Composite	E	ZPE	E <sub>C</sub>
NF+Al(d)	-2354197.67	142.41	-2354055.26
NF+2Al(s)	-2990928.28	137.68	-2990790.60
NF+2Al(t)	-2990809.75	139.33	-2990670.42

In kJ/mol.

Figure 6 display the effect of aluminum on some of the nitroform molecular orbitals.

**Figure 6.** Effect of aluminum on some of nitroform molecular orbitals.

Note that for all the systems considered, except NF and NF+2Al(s) composite each of which stands for a closed-shell structure,  $\alpha$ - and  $\beta$ -type molecular orbitals emerge due to

the unrestricted treatment. In the figure they are represented by notation as a- and b-type molecular orbital energy levels. Each system has its own peculiarities beyond any generalizations. Table 3 shows the HOMO, LUMO energies and the interfrontier molecular orbital energy (FMO) gap values ( $\Delta\varepsilon = \varepsilon_{\text{LUMO}} - \varepsilon_{\text{HOMO}}$ ). The order of HOMO energies is  $\text{NF} < \text{NF} + \text{Al}(\text{d}) < \text{NF} + 2\text{Al}(\text{s}) < \text{NF} + 2\text{Al}(\text{t})$ , whereas the LUMO energies follow the order of  $\text{NF} + \text{Al}(\text{d}) < \text{NF} + 2\text{Al}(\text{t}) < \text{NF} < \text{NF} + 2\text{Al}(\text{s})$ . Thus, the presence of aluminum atom raises up the HOMO energies as compared to nitroform whereas it lowers the LUMO energies except the  $\text{NF} + 2\text{Al}(\text{s})$  case. However, one should keep in mind that  $\text{NF} + 2\text{Al}(\text{s})$  system has a decomposed nitroform structure. The effect of aluminum causes  $\Delta\varepsilon$  values follow the order of  $\text{NF} + 2\text{Al}(\text{t}) < \text{NF} + \text{Al}(\text{d}) < \text{NF} + 2\text{Al}(\text{s}) < \text{NF}$ . On the other hand, the narrowing of interfrontier molecular orbital gap indicates that the composite  $\text{NF} + 2\text{Al}(\text{t})$  should be more sensitive to impact stimuli because  $\Delta\varepsilon$  values are related to impact sensitivity of explosives [37,38]. Namely, as the FMO energy gap ( $\Delta\varepsilon$ ) becomes less and less the impact sensitivity increases more and more. Consequently, aluminum atom makes nitroform to be more susceptible to impact stimulus.

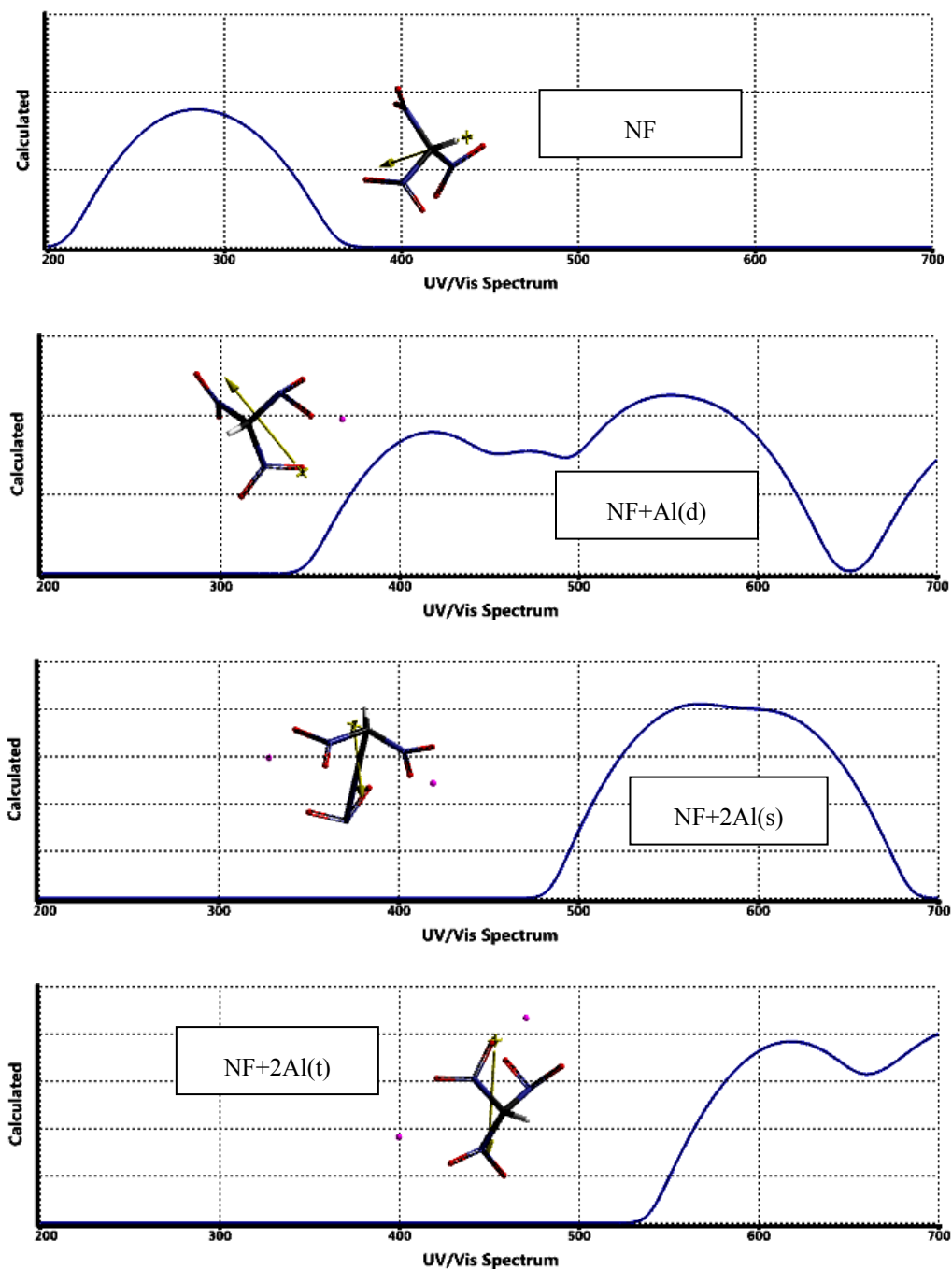
**Table 3.** The HOMO, LUMO energies and the interfrontier molecular orbital energy gap ( $\Delta\varepsilon$ ) values of the systems considered.

Composite	HOMO	LUMO	$\Delta\varepsilon$
NF	-961.03	-399.35	561.68
NF+Al(d)	-651.10	-433.54	217.56
NF+2Al(s)	-640.23	-392.56	247.67
NF+2Al(t)	-609.72	-426.41	183.31

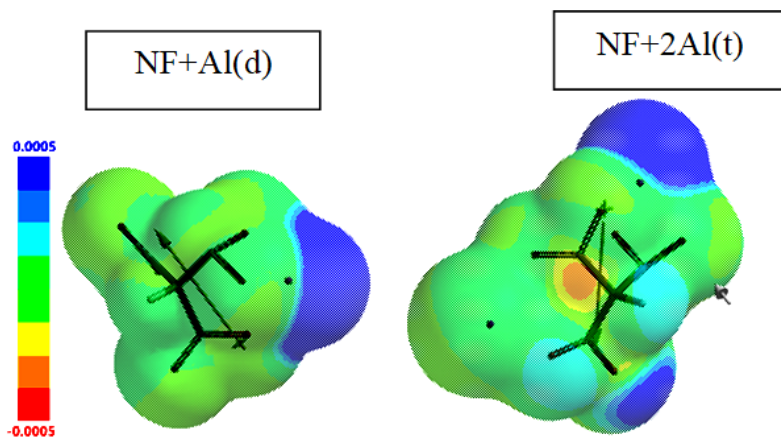
In kJ/mol.

Figure 7 shows the calculated (time-dependent DFT, TDDFT) UV-VIS spectra of the systems considered. As seen in the figure, the presence of aluminum is accompanied by a certain degree of bathochromic shift towards the visible part of the spectrum. The effect is in accord with decreasing value of  $\Delta\varepsilon$  as tabulated in Table 3.

Figure 8 is the spin density maps of the open-shell systems considered. The unpaired electron population in each case has been spread over the whole nitroform moiety but in unequal density. However, the doublet and triplet composites also exhibit some major variations in density.

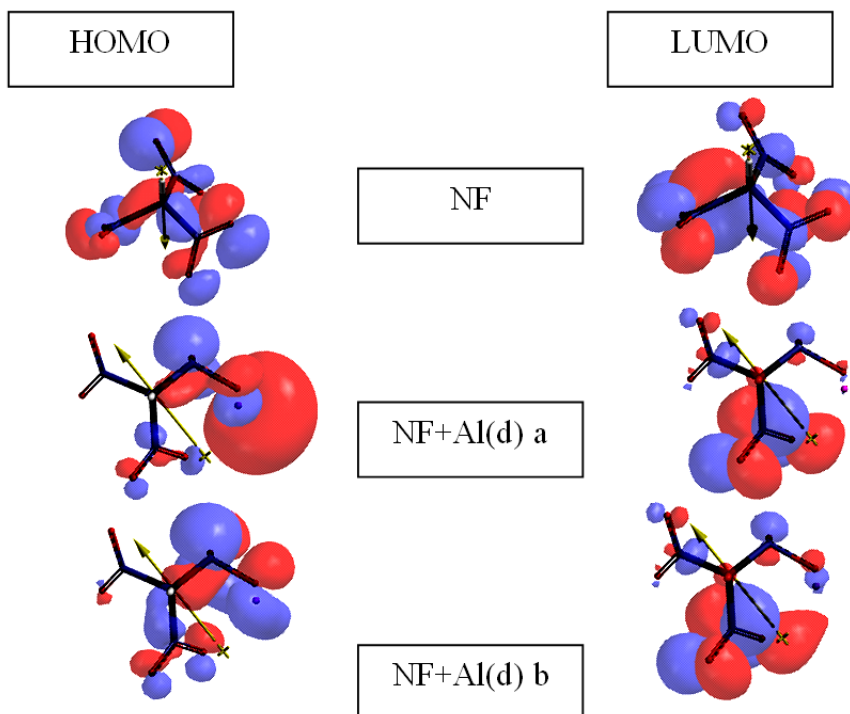


**Figure 7.** Calculated UV-VIS spectra of the systems considered.



**Figure 8.** Spin density maps of the open-shell systems considered.

Figure 9 shows the HOMO and LUMO patterns of NF and the composites considered. Since, unrestricted calculations (UB3LYP/6-311++G(d,p)) have been performed and aluminum atom has an unpaired electron in its ground electronic state, the



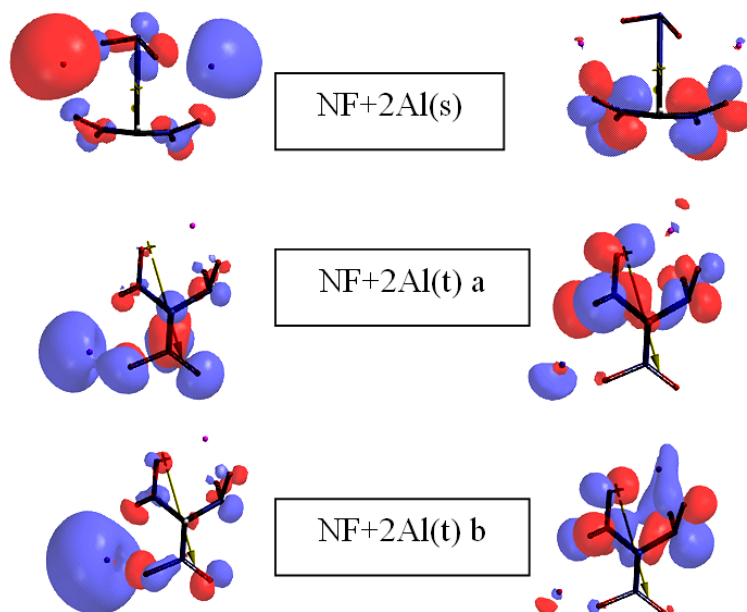


**Figure 9.** The HOMO and LUMO patterns of NF and the composites considered.

composites in the doublet and triplet states considered have  $\alpha$ - and  $\beta$ -HOMO and LUMO orbitals (in the figure those orbitals are designated as a- and b-). As seen in the figure the aluminum atom(s) generally has/have a large contribution to the HOMO while very little or nil in to the LUMO.

#### 4. Conclusion

The present DFT treatment of aluminum and nitroform interaction (within the constraints of the theory and basis set employed) has revealed that aluminum may be compatible or not with nitroform molecule depending on the percent of aluminum in the composite as well as the multiplicity state of the composite. The  $\text{NF}+\text{Al}$  composite is structurally stable but  $\text{NF}+2\text{Al}$  is stable in the triplet but not in the singlet state. In all the cases aluminum atom(s) possesses some partial positive charge.

#### References

- [1] Urbanski, T. (1984). *Chemistry and technology of explosives* (Vol. 4). Oxford: Pergamon, UK. <https://doi.org/10.1002/ijch.196400070>
- [2] Mul, J.M., Gadiot, G.M.H.J.L., Meulenbrugge, J.J., Korting, P.A.O.G., Schnorhk, A.J., &

- Schoyer, H.F.R. (1992). New solid propellants based on energetic binders and HNF. AIAA 1992-3627. *28th Joint Propulsion Conference and Exhibit* (July 1992).  
<https://doi.org/10.2514/6.1992-3627>
- [3] Brown, J.A. (1968). Stabilization of nitroform salts. U.S. Patent 3,378,595 (April 16, 1968).
- [4] Brown, J.A. (1968). Stabilization of nitroform salts. U.S. Patent 3,384,675 (May 21, 1968).
- [5] Louwers, J., & van der Heijden, A.E.D. (1999). Hydrazinium nitroformate. International patent application WO 99/58498.
- [6] Schoyer, H.F.R., Schnorhk, A.J., Korting, P.A.O.G., van Lit, P.J., Mul, J.M., Gadiot, G.M.H.J.L., & Meulenbrugge, J.J. (1995). High performance propellants based on hydrazinium nitroformate. *Journal of Propulsion and Power*, 2, 856-869.  
<https://doi.org/10.2514/3.23911>
- [7] Schoyer, H.F.R., Schnorhk, A.J., Korting, P.A.O.G., & van Lit, P.J. (1997). First experimental results of an HNF/A1/GAP solid rocket propellant. AIAA 1997-3131. *33rd Joint Propulsion Conference and Exhibit* (July 1997).  
<https://doi.org/10.2514/6.1997-3131>
- [8] Low, G.M., & Haury, V.E. (1973). Hydrazinium nitroformate propellant with saturated hydrocarbon binder. U.S. Patent 3,708,359 (January 2, 1973).
- [9] Low, G.M., & Haury, V.E. (1973). Hydrazinium nitroformate propellant stabilized with nitroguanidine. U.S. Patent 3,658,608 (April 25, 1973).
- [10] Bryan, J.C., Burnett, M.N., & Gakh, A.A. (1998). Tetrabutylammonium and caesium salts of trinitromethane. *Acta Cryst. C*, 54, 1229-1233.  
<https://doi.org/10.1107/S0108270198004491>
- [11] Cioslowski, J., Mixon, S.T., & Fleischmann, E.D. (1991). Electronic structures of trifluoro-, tricyano-, and trinitromethane and their conjugate bases. *J. Am. Chem. Soc.*, 113, 4751- 4755. <https://doi.org/10.1021/ja00013a007>
- [12] Ju, X-H., Xiao, J-J., & Xiao, H-M. (2003). DFT Study of the intermolecular interaction of hydrazinium nitroformate ion pair. *Chemical Journal of Chinese Universities*, 24(6), 1067-1071. <http://www.cjcu.jlu.edu.cn/CN/Y2003/V24/16/1067>
- [13] Schoyer, H.F.R., Welland-Veltman, W.H.M., Louwers, J., Korting, P.A.O.G., van der Heijden, A.E.D.M., Keizers, H.L.J., & van den Berg, R.P. (2002). Overview of the development of hydrazinium nitroformate. *Journal of Propulsion and Power*, 18(1), 131-137. <https://doi.org/10.2514/2.5908>

- [14] Dendage, P.S., Sarwade, D.B., Asthana, S.N., & Singh, H. (2001). Hydrazinium nitroformate (HNF) and HNF based propellants: A review. *Journal of Energetic Materials*, 19(1), 41-78. <https://doi.org/10.1080/07370650108219392>
- [15] Dickens, B. (1967). Crystal structure of hydrazine nitroform  $[N_2H_5^+C(NO_2)_3^-]$ . *Chemical Communications*, 5, 246-247. <https://doi.org/10.1039/C19670000246>
- [16] Yan, C., Ding, P., Yang, H., Lu, C., & Cheng, G. (2016). New synthetic route of nitroform (NF) from acetyl acetone and study of the reaction mechanism. *Ind. Eng. Chem. Res.*, 55(41), 11029-11034. <https://doi.org/10.1021/acs.iecr.6b02049>
- [17] Lu, H-Y., Li, J-R., Yang, D-L., Zhang, Q., & Shi, D-X. (2015). A novel synthesis of nitroform by the nitrolysis of cucurbituril. *Chinese Chemical Letters*, 26(3), 365-368. <https://doi.org/10.1016/j.ccllet.2014.12.019>
- [18] Ledgard, J. (2007). *The preparatory manual of explosives* (3rd ed.). Jared Ledgard.
- [19] Davenas, A. (2003). Development of modern solid propellants. *Journal of Propulsion and Power*, 19(6), 1108-1128. <https://doi.org/10.2514/2.6947>
- [20] Schoyer, H.F.R., Korting, P.A.O.G., Veltmans, W.H.M., Louwers, J., van den Heijden, A.E.D.M., Keizers, H.L.J., & van der Berg, R.P. (2000). An overview of HNF and HNF-based propellants. AIAA 2000-3184. *36th AIAA/ASME/SAE/ASEE Joint Propulsion Conference and Exhibit* (July 2000). <https://doi.org/10.2514/6.2000-3184>
- [21] He, Y., Zhang, H., & Lv, M. (2020). The strategy for improving the stability of nitroform derivatives-high-energetic oxidant based on hexanitroethane. *J. Mol. Model.*, 26(7), 181(1-9). <https://doi.org/10.1007/s00894-020-04451-z>
- [22] Taylor, J. (1959). *Solid propellant and exothermic compositions*. London: George Newnes Ltd.
- [23] Keshavarz, M.H. (2005). New method for predicting detonation velocities of aluminized explosives. *Combustion Flame*, 142, 303-307. <https://doi.org/10.1016/j.combustflame.2005.03.011>
- [24] Stewart, J.J.P. (1989). Optimization of parameters for semi empirical methods I. *J. Comput. Chem.*, 10, 209-220. <https://doi.org/10.1002/jcc.540100208>
- [25] Stewart, J.J.P. (1989). Optimization of parameters for semi empirical methods II. *J. Comput. Chem.*, 10, 221-264. <https://doi.org/10.1002/jcc.540100209>
- [26] Leach, A.R. (1997). *Molecular modeling*. Essex: Longman.
- [27] Kohn, W., & Sham, L.J. (1965). Self-consistent equations including exchange and correlation effects. *Phys. Rev.*, 140, 1133-1138. <https://doi.org/10.1103/PhysRev.140.A1133>

- [28] Parr, R.G., & Yang, W. (1989). *Density functional theory of atoms and molecules*. London: Oxford University Press.
- [29] Becke, A.D. (1988). Density-functional exchange-energy approximation with correct asymptotic behavior. *Phys. Rev. A*, *38*, 3098-3100.  
<https://doi.org/10.1103/PhysRevA.38.3098>
- [30] Vosko, S.H., Wilk, L., & Nusair, M. (1980). Accurate spin-dependent electron liquid correlation energies for local spin density calculations: a critical analysis. *Can. J. Phys.*, *58*, 1200-1211. <https://doi.org/10.1139/p80-159>
- [31] Lee, C., Yang, W., & Parr, R.G. (1988). Development of the Colle-Salvetti correlation energy formula into a functional of the electron density. *Phys. Rev. B*, *37*, 785-789.  
<https://doi.org/10.1103/PhysRevB.37.785>
- [32] Cramer, C.J. (2004). *Essentials of computational chemistry*. Chichester, West Sussex: Wiley.
- [33] SPARTAN 06 (2006). Wavefunction Inc.. Irvine CA, USA.
- [34] Göbel, M., & Klapötke, T.M. (2007). Potassium-, ammonium-, hydrazinium-, guanidinium-, aminoguanidinium-, diaminoguanidinium-, triaminoguanidinium- and melaminium nitroformate – synthesis, characterization and energetic properties. *Z. Anorg. Allg. Chem.*, *633*, 1006-1017. <https://doi.org/10.1002/zaac.200700114>
- [35] Türker, L. (2016). Thermobaric and enhanced blast explosives (TBX and EBX). *Defence Technology*, *12*(6), 423-445. <https://doi.org/10.1016/j.dt.2016.09.002>
- [36] Durant, P.J., & Durant, B. (1972). *Introduction to advanced inorganic chemistry*. London: Longman.
- [37] Anbu, V., Vijayalakshmi, K.A., Karunathan, R., Stephen, A.D., & Nidhin, P.V. (2019). Explosives properties of high energetic trinitrophenyl nitramide molecules: A DFT and AIM analysis. *Arabian Journal of Chemistry*, *12*(5), 621-632.  
<https://doi.org/10.1016/j.arabjc.2016.09.023>
- [38] Badders, N.R., Wei, C., Aldeeb, A.A., Rogers, W.J., & Mannan, M.S. (2006). Predicting the impact sensitivities of polynitro compounds using quantum chemical descriptors. *Journal of Energetic Materials*, *24*, 17-33. <https://doi.org/10.1080/0737065050037432>